Journal of the Physical Society of Japan
Vol. 73, No. 4, April, 2004, pp. 1090–1091

Successive Change of Phase Transition Character in Lead Zinc Niobate Titanate Single Crystals

Bijun FANG*, Yuejin SHAN*, Hideo IMOTO, Haiqing XU[1], Haosu LUO[1] and Zhiwen YIN[1]

Department of Applied Chemistry, Faculty of Engineering, Utsunomiya University, 7-1-2 Yoto, Utsunomiya 321-8585
[1]*The State Key Laboratory of High Performance Ceramics and Superfine Microstructure, Shanghai Institute of Ceramics, Chinese Academy of Sciences, Shanghai 201800, China*

(Received January 13, 2004)

KEYWORDS: lead zinc niobate titanate, crystal structure, dielectric property, ferroelectric property, phase transition

DOI: 10.1143/JPSJ.73.1090

$(1-x)$Pb$(Zn_{1/3}Nb_{2/3})O_3$–xPbTiO$_3$ ($(1-x)$PZN–xPT) single crystal with a composition near the morphotropic phase boundary (MPB, $x = 0.08$–0.105) exhibits excellent electrical property,[1,2] which makes it a promising candidate for the next generation electromechanical transducer application.[3,4] $(1-x)$PZN–xPT is relatively easy to grow in single crystal form by a fluxing method over the whole composition range. However, the fluxing method is unsuitable for growing large crystals due to its poor reproducibility and the occurrence of spontaneous nucleation. By comparison, the Bridgman method can obtain excellent reproducibility and large productivity by introduction a seed crystal into crystal growth.[5,6]

In this note, $(1-x)$PZN–xPT single crystals with composition $x = 0.05$, 0.09 and 0.15 were grown by a modified Bridgman method using an allomeric Pb$[(Mg_{1/3}Nb_{2/3})_{0.69}$-$Ti_{0.31}]O_3$ (PMNT 69/31) single crystal as a seed.[7] The phase transition behavior dependence on composition of the as-grown $(1-x)$PZN–xPT crystals were discussed.

Lattice structure of the $(1-x)$PZN–xPT crystals was investigated by X-ray diffraction measurement (XRD, Rigaku D/MAX-3C) using ground crystals. The obtained crystals are of pure perovskite phase and the crystal structure changes from rhombohedral in PZNT95/5, through coexistence of rhombohedral and tetragonal in PZNT91/9, and to tetragonal in PZNT85/15 with the increase of $PbTiO_3$ content. Table I shows the lattice parameters of the $(1-x)$PZN–xPT crystals calculated by the least-squares method. The lattice parameters of the PZNT91/9 crystal were calculated on a rhombohedral unit cell due to its slight tetragonal distortion. It can be seen that the PZNT91/9 crystal can be pictured as providing a "bridge" between the rhombohedral and tetragonal structures since its cell is similar to both the rhombohedral and tetragonal lattices.

Dielectric property of the $(1-x)$PZN–xPT crystals was measured by a computer-interfaced analyzer (HP4192A). Figure 1 shows temperature dependence of the dielectric constant of the $(1-x)$PZN–xPT crystals. There is just one unique anomaly in the PZNT95/5 crystal, where the temperature of dielectric peaks (T_m) appears at around 140°C accompanied with apparent frequency dispersion. T_m increases from 138.1°C at 120 Hz to 144.6°C at 100 kHz,

Table I. Lattice parameters of the $(1-x)$PZN–xPT single crystals.

Composition	a/Å	b/Å	c/Å	α/°	β/°	γ/°
PZNT95/5	4.1062	4.1062	4.1062	91.52	91.52	91.52
PZNT91/9	4.0195	4.0195	4.0195	89.31	89.31	89.31
PZNT85/15	4.0152	4.0152	4.0971	90.00	90.00	90.00

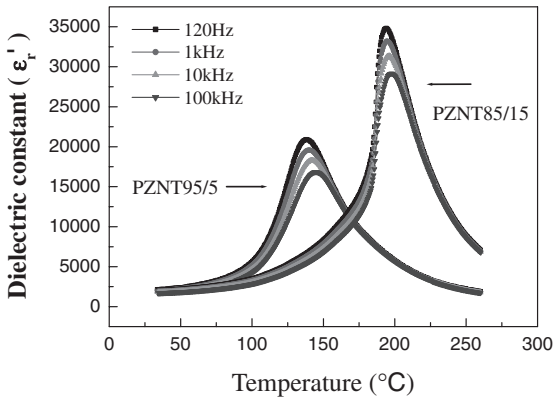

Fig. 1. Temperature dependence of the dielectric constant measured at different frequencies upon heating of the $(1-x)$PZN–xPT crystals (001) planes.

whereas the maximum value of dielectric constant (ε_m) decreases from 20921 to 16842. The full-width-at-half-maximum (FWHM) of the dielectric peaks is around 50°C, which shows the nature of a relaxor. As a comparison, a relatively sharp dielectric anomaly appears in the PZNT85/15 crystal at about 200°C, which indicates the crystal changes to normal ferroelectric (FE).

The relaxor nature of the $(1-x)$PZN–xPT crystals can be described by a quadratic law, which was a modified Curie–Weiss law proposed by Uchino *et al.*:[8]

$$1/\varepsilon = 1/\varepsilon_{max} + (T - T_{max})^n/C' \quad (1)$$

where n is a diffuseness index and C' is a constant. The diffuseness index can be solved graphically by eq. (1) using a log–log plot as illustrated in Fig. 2. The slope of the curve represents the value of the diffuseness index, while the intercept gives the diffuseness parameter by following equation:

$$\delta = (e^{-\text{intercept}}/2\varepsilon_{max})^{1/n} \quad (2)$$

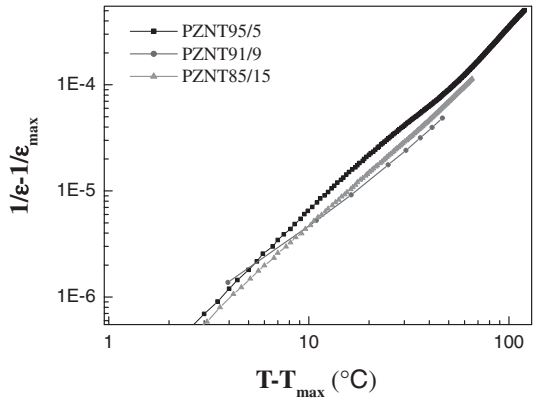

Fig. 2. Plot of $\log(1/\varepsilon - 1/\varepsilon_{max})$ vs $\log(T - T_{max})$ of the $(1-x)$PZN–xPT single crystals.

*E-mail: fangbj@sohu.com

Table II. Dielectric properties of the $(1-x)$PZN–xPT single crystals using 1 kHz data.

Composition	T_{max}/°C	ε_{max}	ΔT/°C 100 Hz–100 kHz	n	δ/°C	$C'/\times 10^5$	R^2
PZNT95/5	140.2	19586.0	6.5	1.73	22.84	89.128	0.9981
PZNT91/9	177.6	50580.6	0.0	1.45	16.26	57.058	0.9977
PZNT85/15	194.7	33212.4	3.8	1.70	20.28	112.289	0.9997

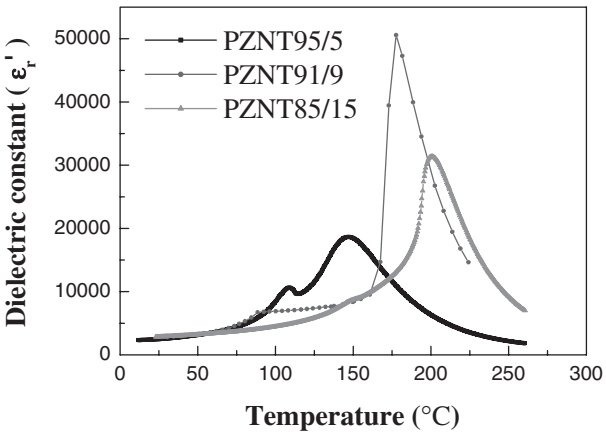

Fig. 3. Temperature dependence of the dielectric constant of the poled $(1-x)$PZN–xPT crystals (001) planes at 1 kHz upon heating.

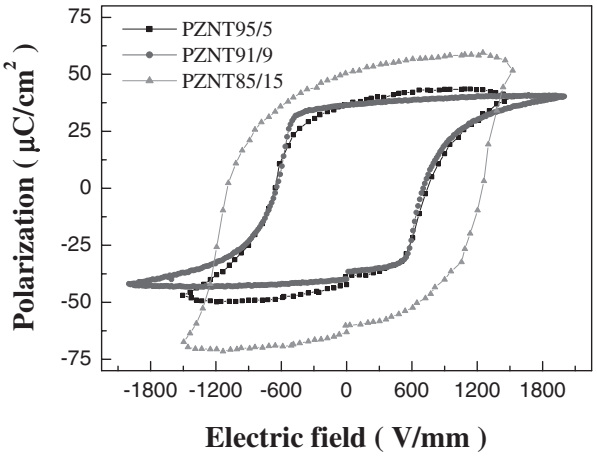

Fig. 4. Electric hysteresis loops of the $(1-x)$PZN–xPT crystals (001) planes.

Table II lists the results of a linear regression analysis of the data shown in Fig. 2. The PZNT85/15 crystal also exhibits slight frequency dispersion, which can be attributed to the variation of composition caused by segregation during crystal growth and partly to the disorder distribution of ions at the B-sites of perovskite structure.

Figure 3 shows the influence of polarization on the dielectric response of the $(1-x)$PZN–xPT crystals. (Polarization was carried out under 1 kV/mm at 150°C for 15 min in silicon oil.) In the PZNT91/9 crystal, the character of dielectric response retains except for a slight change of the values of ε_m and T_m after poling. However, in the PZNT95/5 crystal, an additional dielectric anomaly appears at 109.0°C, which can be attributed to the formation of macro domain or induced tetragonal FE domain. No frequency dispersion appears in this temperature range, while the dispersion of the original dielectric anomaly becomes severe. The values of T_m and ε_m change greatly from 140.2°C and 19586.0 to 147.1°C and 18663.0 after poling at 1 kHz, respectively. In the PZNT85/15 crystal, a dielectric shoulder appears at a lower temperature of 150.0°C, which is regarded as correlating with the orientation of tetragonal FE domain. Polarization increases the stabilization of FE domain, which leads to the temperature of FE phase transition moving to a high temperature. The growth and orientation of FE domain induced by poling decrease the contribution of domain wall movement on the dielectric response, which leads to the decrease of the value of maximum dielectric constant.

Figure 4 shows the ferroelectric hysteresis loops of the $(1-x)$PZN–xPT crystals (001) planes measured by a RT-66A Standard Ferroelectric Test System (Radiant Tech. Inc.). The PZNT85/15 crystal exhibits slightly large saturation polarization that is due to the easy movement of the tetragonal FE domain under external electric field along the spontaneous polarization direction.

In summary, the PZNT95/5 crystal possesses a diffused ferroelectric transition since a broad dielectric peak accompanied with obvious frequency dispersion appears in the dielectric response. Polarization not only induces an additional dielectric anomaly, but also leads to the appearance of irregular, fine macro-domain observed by light observation. The phase transitions in the PZNT91/9 crystal are a nearly first-order transition with slight diffuse character.[1,2,7] For the PZNT85/15 crystal there exhibits just one unique anomaly in the dielectric response again, where thermal hysteresis is obvious and frequency dispersion exhibits slightly. Therefore, the PZNT85/15 crystal approaches to a normal ferroelectric.

Acknowledgements

The authors would like to thank the National Natural Science Foundation of China and the Shanghai Municipal Government for financial support.

1) K. Harada, S. Shimanuki, T. Kobayashi, S. Saitoh and Y. Yamashita: J. Am. Ceram. Soc. **81** (1998) 2785.
2) J. Kuwata, K. Uchino and S. Nomura: Jpn. J. Appl. Phys. **21** (1982) 1298.
3) S. Saitoh, T. Kobayashi, K. Harada, S. Shimanuki and Y. Yamashita: IEEE Trans. Ultrason. Ferroelectr. Freq. Control **45** (1998) 1071.
4) T. Kobayashi, S. Shimanuki, S. Saitoh and Y. Yamashita: Jpn. J. Appl. Phys. **36** (1997) 6035.
5) S. Shimanuki, S. Saito and Y. Yamashita: Jpn. J. Appl. Phys. **37** (1998) 3382.
6) K. Harada, Y. Hosono, S. Saitoh and Y. Yamashita: Jpn. J. Appl. Phys. **39** (2000) 3117.
7) B. Fang, H. Xu, T. He, H. Luo and Z. Yin: J. Cryst. Growth **244** (2002) 318.
8) K. Uchino and S. Nomura: Ferroelectr. Lett. **44** (1982) 55.